Scaling relations between anomalous Hall and longitudinal transport coefficients in metallic (Ga,Mn)As films

Xinyu Liu, S. Shen, Z. Ge, W. L. Lim, M. Dobrowolska, J. K. Furdyna, and Sanghoon Lee

Temperature Dependence of Anomalous Hall Effect in Metallic (Ga,Mn)As films: a Study of Scaling Relation

Xinyu Liu,[*] S. Shen, Z. Ge, W. L. Lim, M. Dobrowolska, and J. K. Furdyna

Department of Physics, University of Notre Dame, Notre Dame, IN 46556, USA

Sanghoon Lee[†]

Physics Department, Korea University, Seoul 136-701, KOREA

(Dated: March 1, 2011)

We report a systematic study of the temperature dependence of the anomalous Hall and longitudinal conductivities σ_{xy} and σ_{xx} and resistivities ρ_{xy} and ρ_{xx} in a series of metallic (Ga,Mn)As samples. Two universal scaling relations are obtained: $\sigma_{xy} \propto \sigma_{xx}^{1.5}$, obtained from measurements at a fixed low temperature (2.0 K) on a series of samples with different Mn concentrations; and $\rho_{xy}/m \propto \rho_{xx}^2$, where m is normalized magnetization, obtained from the temperature variation of ρ_{xx} and ρ_{xy} measured on each sample of the series. The former scaling relation is, however, found to break down for highly conducting (Ga,Mn)As samples ($\sigma_{xx} > 100\ \Omega^{-1}\text{cm}^{-1}$). The latter scaling relation leads to a magnetization-dependent anomalous Hall coefficient, which we attribute to the emergence of magnetization fluctuations at high temperatures.

PACS numbers: 75.47.-m, 75.50.Pp, 72.25.Dc, 72.15.Rn
Keywords: ferromagnetic semiconductor, (Ga,Mn)As, anomalous Hall effect, conductivity, scaling relations

I. INTRODUCTION

A. Background and motivation

The study of Hall resistivity ρ_{xy} of ferromagnetic metals and semiconductors, as well its linear and quadratic dependence on the longitudinal resistivity ρ_{xx} (i.e., the scaling relation between ρ_{xy} and ρ_{xx} is one of most interesting subjects in magnetotransport in ferromagnetic materials, since it can lead to an understanding of the mechanisms that contribute to the anomalous Hall effect (AHE), including its relation to spin polarization and spin-orbit coupling of charge carriers. It is usually assumed that AHE caused by magnetic moments embedded in a ferromagnetic metal[1] may arise from *extrinsic* scattering processes involving spin-orbit coupling: specifically, skew scattering[2] and/or side-jump processes[3]. Recently, however, AHE has reemerged as an active area of both theoretical[4–7] and experimental[8–14] research, owing to the introduction of an additional *intrinsic* mechanism for AHE that involves the interaction of carrier spins with the inherent spin-orbit-coupled Bloch bands[5,15–19].

Despite extensive studies of this problem, the identification of the microscopic origins responsible for AHE in magnetic materials obtained by analyzing the scaling relation between the anomalous Hall and the longitudinal resistivities $\rho_{xy} \propto \rho_{xx}^n$ is still a challenging task. This is especially true in the case of ferromagnetic semiconductors such as (Ga,Mn)As, where the exponent $n = 2$ reported in Refs. 9 and 19 applies to both intrinsic and side-jump mechanisms, making it difficult to distinguish between the two processes; and also given the fact that Mn atoms in these materials act simultaneously as the source of magnetic moments and as acceptors, which complicates the analysis of scattering processes in this material. Furthermore, several recent studies of (Ga,Mn)As samples have reported a universal empirical scaling relation between the anomalous Hall and the longitudinal conductivities $\sigma_{xy} \propto \sigma_{xx}^\gamma$ with γ of about 1.6, which holds over a wide range of conductivities (between 0.01 and 100 $\Omega^{-1}\text{cm}^{-1}$)[13,14,20]. By very simple algebra (see Sec. IB) it can be readily shown that $\rho_{xy} \propto \rho_{xx}^2$ and $\sigma_{xy} \propto \sigma_{xx}^{1.6}$ cannot apply simultaneously under conditions where AHE is dominant. It is therefore necessary to examine these two apparently contradictory scaling relations carefully, in order to develop a clear and complete scheme for carrier transport in (Ga,Mn)As.

We note parenthetically that the determination of the hole concentration p in (Ga,Mn)As, while it is critically important for our understanding of ferromagnetism in this material, is made difficult in practice precisely because the ordinary Hall term in the Hall measurement is obscured by AHE. Thus a clear picture of the scaling characteristics of the dominant AHE term in ρ_{xy} becomes additionally important for the process of extracting the value of p from the Hall data.

B. Formal description of AHE and relevant approximations

Since magneto-transport measurements directly provide the values of ρ_{xy} and ρ_{xx}, but in certain circumstances it is more informative to discuss the results in term of σ_{xy} and σ_{xx}. In this section we briefly review the inverse relations between the $\boldsymbol{\rho}$ and $\boldsymbol{\sigma}$ tensors. In ferromagnetic systems, the Hall resistivity is often described as a sum of two terms,

$$\rho_{xy} = R_0 B + R_S M, \tag{1}$$

an ordinary Hall contribution due to the Lorentz force, plus an anomalous Hall term that is proportional to the magnetization M. In Eq. (1) B and M are components of the applied field and the magnetization perpendicular to the current (i.e., in the case of thin films, normal to the film plane); and R_0 and R_S are the normal and anomalous Hall coefficients, respectively. A similar separation as in Eq. (1) can be made in the Hall conductivity,

$$\sigma_{xy} = \sigma_0 \mu B + \chi_S M, \tag{2}$$

where σ_0 is zero-field conductivity and μ is the carrier mobility. The first term in Eq. (2) corresponds to the ordinary Hall effect related to carrier concentration, while the second term defines the anomalous Hall conductivity proportional to magnetization, χ_S being a coefficient. Note that the electrical conductivity tensor $\boldsymbol{\sigma}$ is the inverse of the electrical resistivity tensor $\boldsymbol{\rho}$ with the relations between the diagonal and off-diagonal components give by

$$\begin{aligned} \sigma_{xx} &= \rho_{xx}/(\rho_{xx}^2 + \rho_{xy}^2), \\ \sigma_{xy} &= \rho_{xy}/(\rho_{xx}^2 + \rho_{xy}^2). \end{aligned} \tag{3}$$

Since in most ferromagnets – including metallic (Ga,Mn)As – the Hall resistivity ρ_{xy} is at least one order of magnitude smaller than the longitudinal resistivity ρ_{xx}, the Hall conductivity reduces to

$$\sigma_{xy} \approx \rho_{xy}/\rho_{xx}^2. \tag{4}$$

Finally, when the carrier mobility satisfies the inequality $\mu B \ll 1$, characteristic for (Ga,Mn)As for values of B used in this study, we can write

$$\sigma_{xx} \approx 1/\rho_{xx}. \tag{5}$$

In (Ga,Mn)As with the Mn concentrations exceeding 0.5% (representing the samples used in this study) the contribution of the ordinary Hall effect is typically much smaller than the AHE term, and can be neglected. Under these conditions we have

$$\begin{aligned} \rho_{xy} &\approx R_S M, \\ \sigma_{xy} &\approx \chi_S M \approx R_S M/\rho_{xx}^2, \end{aligned} \tag{6}$$

yielding the relation between the anomalous Hall coefficients $\chi_S \approx R_S/\rho_{xx}^2$. From Eqs. (4)-(6) it follows directly that – as already mentioned – the two scaling relations $\sigma_{xy} \propto \sigma_{xx}^{1.5}$ and $\rho_{xy} \propto \rho_{xx}^2$ are contradictory, and thus cannot hold simultaneously. We will return to this issue in Sec. III D.

C. Outline

In this work we report a systematic magnetotransport study of the dependence of ρ_{xy} and ρ_{xx} on temperature and Mn concentration observed in a series of metallic (Ga,Mn)As samples. Based on the obtained results, we then establish the scaling relation between σ_{xy} and σ_{xx} using transport data taken on a series of samples with different Mn concentrations at a fixed low temperature; and scaling relations between ρ_{xy} and ρ_{xx} using their temperature variation obtained for each individual sample in the series. The two scaling relations found in this way are: $\sigma_{xy} \propto \sigma_{xx}^{\gamma}$ with $\gamma \sim 1.5$, and $\rho_{xy} \propto \rho_{xx}^n$ with $n = 2$. Surprisingly, these two distinct and apparently contradictory relations are found to coexist in the intermediate conductivity regime, i.e., in (Ga,Mn)As where the hole concentration p ranges from 2.8×10^{19} cm^{-3} to 10^{20} cm^{-3}; and do not show a smooth progression from one conductivity regime to the other. It is therefore especially important to examine these relationships explicitly as a function of p, and we will do this in detail beginning with Sec. III A.

Moreover, we confirm the results reported in Ref. 14 that the scaling relation of $\sigma_{xy} \propto \sigma_{xx}^{1.5}$ breaks down for highly conducting (Ga,Mn)As samples ($\sigma_{xx} > 100 \ \Omega^{-1}\text{cm}^{-1}$), while the relation of $\rho_{xy} \propto \rho_{xx}^2$ exhibits a magnetization dependent anomalous Hall coefficient. We attribute the latter behavior to the emergence of anomalous Hall effect contributions induced by magnetization fluctuations at high temperatures, including temperatures above T$_C$. The interplay between these scaling relations will be addressed and discussed in terms of the Anderson-Mott metal-insulator transition[21] in Sec. III.

II.   SAMPLE FABRICATION AND EXPERIMENTAL PROCEDURE

All samples in this study were grown by molecular beam epitaxy (MBE) on "epi-ready" semi-insulating GaAs (001) substrates. After thermal cleaning of the substrates, 100 nm thick GaAs buffer layers were first grown at 580°C. The substrate temperature T_s was then reduced to 250°C, and a series of (Ga,Mn)As samples were grown at this temperature as follows. A 2 nm thick GaAs buffer layer was deposited first, followed by the growth of $Ga_{1-x}Mn_xAs$ layers of desired thicknesses between 10 nm and 100 nm. The Mn concentration in each sample was determined by direct readings of the Mn flux in the MBE chamber, and confirmed after the growth by lattice constant measurements by X-ray diffraction. Pieces of the samples were also annealed in the atmosphere of N_2 gas at the temperature of 280°C for 1.0 hour, and subsequently cooled by a rapid quench to room temperature. The samples (both as-grown and annealed) described above were characterized by magneto-transport measurements using the six-probe Hall geometry with indium ohmic contacts in a Janis continuous helium flow cryostat equipped with a superconducting magnet system, allowing us to sweep the magnetic field up to 6 T at various temperatures between 2 and 300 K. The hole concentration in the samples was determined from magneto-transport data obtained at low temperature (< 10 K) using a method described in Ref. 20. The Curie temperatures of the samples were obtained from SQUID magnetization data. A total of ten (Ga,Mn)As samples with Mn concentrations between 3.9% and 6.0% are studied in this work. The characteristics of the samples used in this study are summarized in Table I. We have noticed that, although the relation between the carrier concentration and the Curie temperature $T_C \approx p^1/3$ introduced by Ku et al.[22,23] provides a good semi-quantitative guide for the behavior of T_C, there can exist significant deviations from this trend in any (Ga,Mn)As sample series owing to the complex competing effects between substitutional and interstitial Mn ions[24,25], and the fact that the relative concentrations of these two types of ion can strongly vary from sample to sample due to differences in MBE growth conditions. In addition, it is relevant to note the effect of thickness in this context, i.e., annealing is much more efficient in thinner samples, leading to larger increase in both the effective Mn concentration and in T_C.

TABLE I: Parameters for the (Ga,Mn)As samples used in this study. Symbol @ stands for "annealed". The exponent n obtained for the scaling relation $\rho_{xy}/m \propto \rho_{xx}^n$ is also listed.

Sample #	t (nm)	Mn (x)	p (10^{20}cm^{-3})	n (T<10K)	T_C (K)	Fig. 5
40216C	99	5.2%	1.75	1.82	60	
40218A	97	6.7%	1.24	1.8	68	
50522A	95	3.9%	0.93	1.8	60	
50522A@	95	3.9%	2.55	1.8	80	
50522B	42	3.9%	0.36	1.8	60	a
50522B@	42	3.9%	2.02	1.815	95	b
50523B	20	5.0%	0.74	1.78	60	c
50523B@	20	5.0%	3.17	1.81	110	d
50824C	10	6.0%	0.54	1.41	70	e
50824C@	10	6.0%	7.34	2	132	f

III.   EXPERIMENTAL RESULTS

A.   Scaling relations of σ_{xy} and σ_{xx} at low temperatures

All samples studied show metallic behavior, i.e., a finite conductivity σ_{xx} exists as temperature approaches zero. It is instructive to examine the conductivity σ_{xx} as a function of the hole concentration p, since that is the quantity that ultimately connects σ_{xx}, σ_{xy}, and – it should be emphasized – also the magnetization M. We begin with a log-log plot of σ_{xx} vs. p shown in Fig. 1. While the plot does not indicate any power relation between σ_{xx} and p, it clearly undergoes a dramatic change at $p_c \approx 2.8 \times 10^{19}$ cm^{-3} (marked as p_c in the figure). This point corresponds to the metal-insulator (Anderson-Mott) transition, representing the lower limit of p at which (Ga,Mn)As shows metallic behavior. Having established p_c as the onset of the metallic range, it is logical to use this point as the origin when discussing metallic (Ga,Mn)As, i.e., to use $(p - p_c)$ as the hole concentration variable for that range.

In Fig. 2 we summarize our data for longitudinal and transverse conductivities σ_{xx} and σ_{xy} (at $T = 2$ K) as a function of the variable $(p-p_c)$. Clearly the conductivity σ_{xx} follows a power law as a function of $(p-p_c)$ in the form $\sigma_{xx} \sim (p - p_c)^s$, where $s \approx 0.5$. Such critical behavior, i.e., a power law behavior at the critical region, is commonly
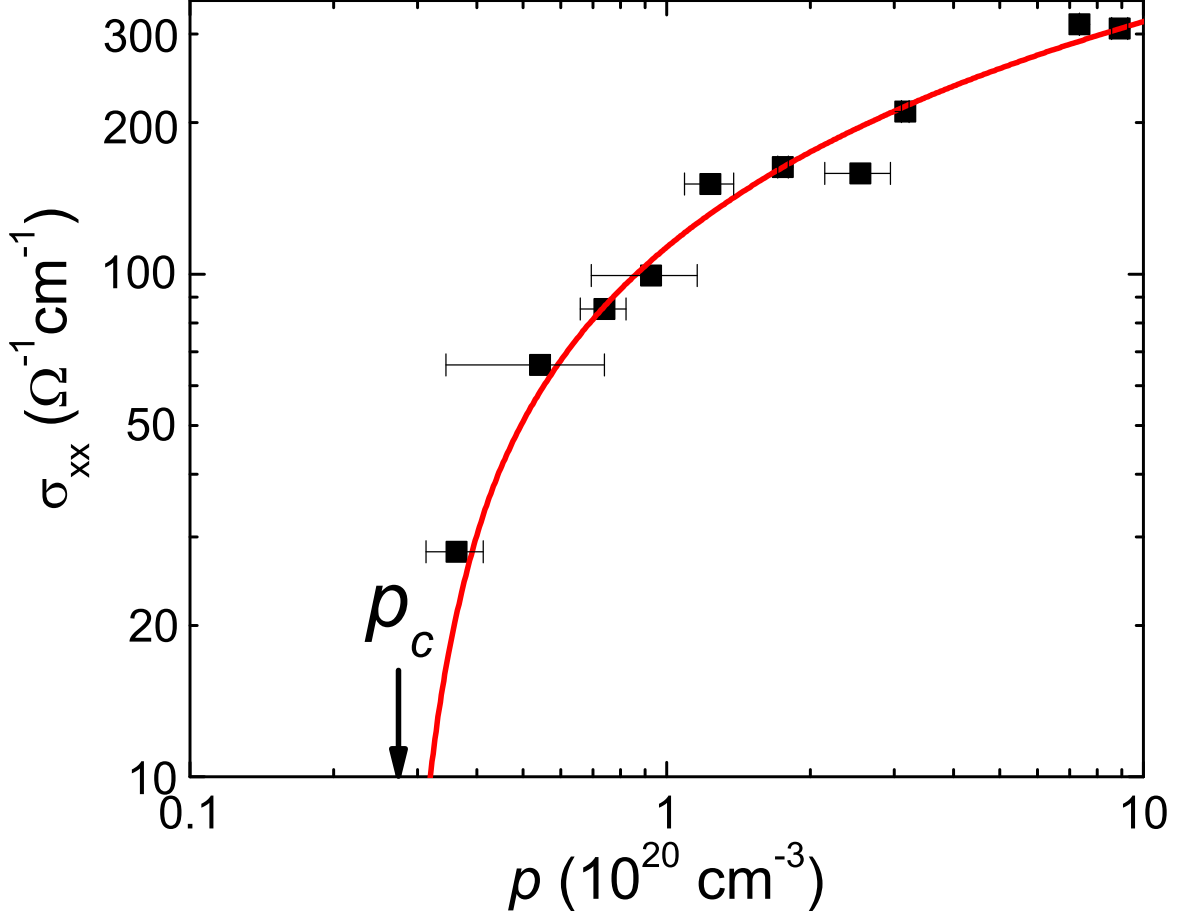
FIG. 1: (Color online) Longitudinal conductivity σ_{xx} vs. hole concentration p at 2 K. The red curve is a guide for the eye. p_c marked in the figure is the metal-insulator transition point.

observed in studies of the Anderson-Mott metal-insulator transition in doped semiconductor systems[26,27]. Although one theoretically expects the exponent s to be ~ 1.0[28,29], our best fit gives a significantly different result, $s \approx 0.5$. A possible explanation for this discrepancy is that the scaling theory applies to the *immediate proximity* of the critical point $p = p_c$, and our data lies too far outside that immediate for the scaling theory to apply[30,31].

As shown in Fig. 2(b), we find that – in contrast to σ_{xx} – the anomalous Hall conductivity σ_{xy} vs. hole concentration has two distinct ranges. For low hole concentration ($p-p_c < 1 \times 10^{20}$ cm^{-3} in Fig. 1), σ_{xy} increases as p increases above the critical point, which shows a similar critical behavior as for σ_{xx}, i.e., a power law relation of $\sigma_{xy} \sim (p - p_c)^{0.76}$. As a result, despite the fact that particular samples may differ in magnetization values, we observe a universal scaling relation $\sigma_{xy} \propto \sigma_{xx}^\gamma$ with $\gamma \sim 1.5$ (or $\rho_{xy} \propto \rho_{xx}^{0.5}$ based on Eq. (4))[32] over low p range up to 10^{20} cm^{-3} (i.e., the intermediate conductivity range, with σ_{xx} up to 100 Ω^{-1}cm^{-1}), in agreement with the value $\gamma \sim 1.5$ reported by Shen *et al.*[20] and the value $\gamma \sim 1.6$ reported by Glunk *et al.*[13], and Chiba *et al.*[14] It should be emphasized that such scaling relation also extends to the localized regimes studied by Shen *et al.*[20] (i.e., down to 0.5 Ω^{-1}cm^{-1}). However, this scaling relation breaks down rather severely in the case of higher hole concentrations (i.e., higher conductivity, $\sigma_{xx} > 100$ Ω^{-1}cm^{-1}), consistent with the recent experiments of Glunk *et al.*[13] and Chiba *et al.*[14] The above behavior agrees with a unified theory of the AHE developed by Onoda *et al.*[33,34], which predicts three regimes that depend on the carrier scattering time: the "clean" regime, where $\rho_{xy} \propto \rho_{xx}$ (not achievable in (Ga,Mn)As); the "intermediate"
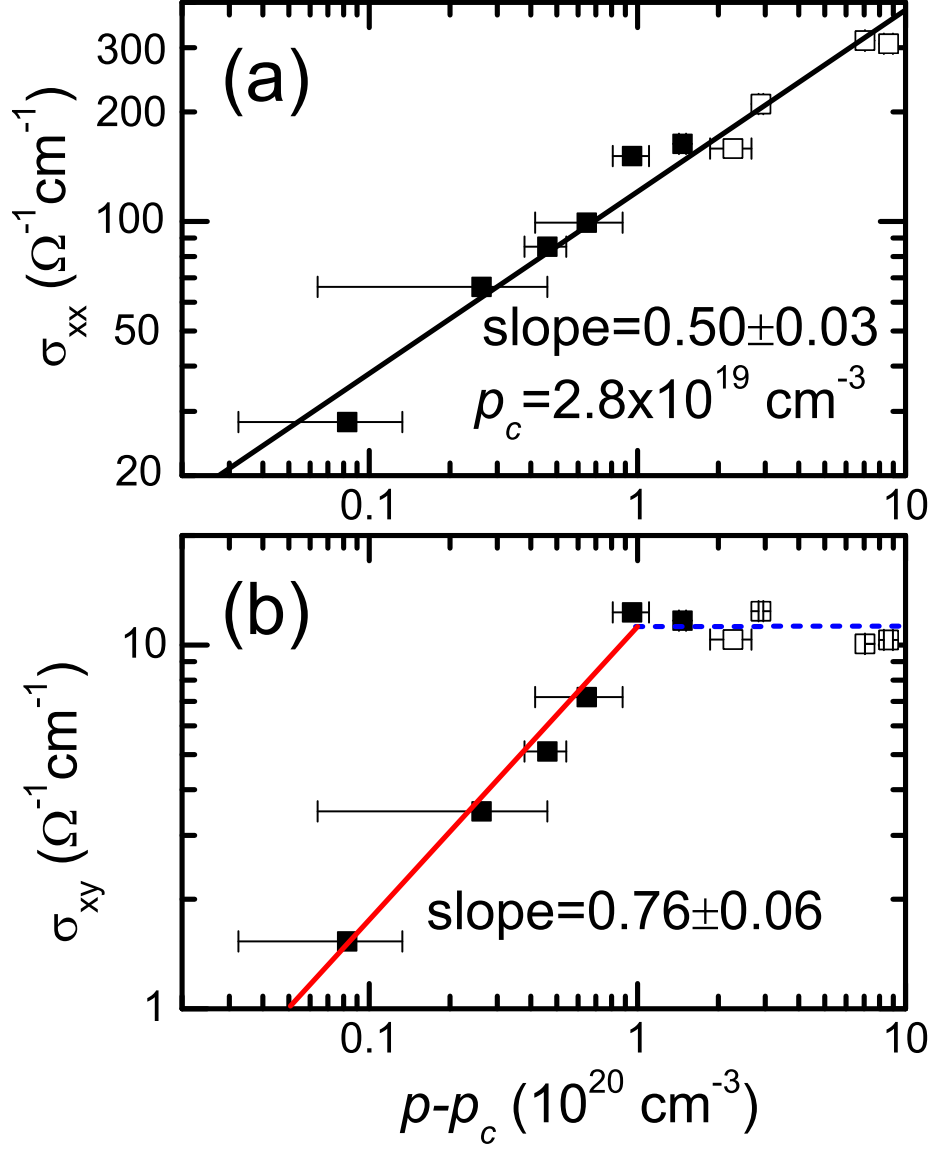
FIG. 2: (Color online) The longitudinal and transverse conductivities σ_{xx} and σ_{xy} vs. hole concentration from metal-insulator transition point, $p - p_c$, at 2 K. The data from the as-grown samples are shown by full symbols, while the open symbols are for the annealed samples. (a) The solid line represents the best power-law fit with $s = 0.50\pm0.03$. (b) The solid line represents the best power-law fit with slope of 0.76 ± 0.06. The dash line is a guide for the eye.

regime, where $\rho_{xy} \propto \rho_{xx}^2$; and the "dirty" regime, for which this theory predicts $\rho_{xy} \propto \rho_{xx}^{0.4}$.

B. Temperature dependence of σ_{xx} and σ_{xy}

We now address the scaling relation between longitudinal and transverse conductivities, σ_{xx} and σ_{xy} (and equivalently, between ρ_{xx} and ρ_{xy}), obtained from temperature dependent measurements. In Figs. 3(a) and 3(b) we first show ρ_{xx} and ρ_{xy} as function of temperature in the range 2 to 300 K for a typical metallic (Ga,Mn)As sample at

several magnetic fields. As previously reported by several groups[35,36], the temperature dependence of ρ_{xx} shows a signature cusp at T_C, which shifts to higher temperatures when a magnetic field is applied. From Fig. 3(a) one can clearly see that the resistivity ρ_{xx} also shows an upturn at lower temperatures (< 10 K). In addition, strong magneto-resistance is observed at temperatures corresponding to the ferromagnetic state, with a maximum around T_C. In contrast to ρ_{xx}, the transverse resistivity ρ_{xy} depends only weakly on temperature and magnetic field below T_C, but above T_C drops rapidly with temperature and shows a pronounced field dependence. It should be especially emphasized that there is a weak cusp in the temperature variation of ρ_{xy} around T_C, which is commonly observed in metallic (Ga,Mn)As samples, but not in insulating samples.

For an individual (Ga,Mn)As sample, the scaling relation between ρ_{xx} and ρ_{xy} can be obtained using the temperature variation of transport data at low temperature and high field, where one can assume that the magnetization is fully saturated[20]. However, the conspicuous difference in the temperature and field dependences of ρ_{xx} and ρ_{xy} shown in Figs. 3(a) and 3(b) clearly suggests that this scaling relation between ρ_{xx} and ρ_{xy} (if it exists) will break down at high temperature. In this regard, the scaling relation $\sigma_{xy} \propto \sigma_{xx}^{1.5}$ (which is equivalent to $\rho_{xy} \propto \rho_{xx}^{0.5}$) will be only valid as the temperature approaches zero, but it should not be applicable at high temperatures.

For better understanding of mechanisms present in this process, it is helpful to examine the temperature variation of σ_{xx} and σ_{xy} in addition to ρ_{xx} and ρ_{xy}. In Fig. 4(a), the σ_{xx} vs. temperature at field of 6 T is plotted as solid black square symbols. Based on a scaling theory for strongly disordered ferromagnets, the temperature variation of σ_{xx} can be understood in terms of the microscopic conductance $g_0(m)$ of a small coherent cube of size $\sim \xi_0$ and a length scale parameter $\xi(T)$[36], where m is the normalized magnetization, defined by

$$m(T, B) = M(T, B)/M_0. \tag{7}$$

In Fig. 4(a), for purposes of illustration we use a *simplified* model in which $\xi(T)$ is only a function of $T^{-1/2}$ which accounts for the electron-electron interaction[37], but does not depend on m[38]. As a result, σ_{xx} can be decomposed into three parts: a constant C, a magnetization dependent term $A(m)$ related to scattering on spin disorder, and a temperature dependent term $B(T)$, as follows

$$\begin{aligned} \sigma_{xx} &= C + A(m) + B(T) \\ &= const. + am^2 + bT^{-1/2}. \end{aligned} \tag{8}$$

where a and b are fitting parameters. Note that am^2 also implicitly depends on T through the magnetization, and that the temperature dependence of $bT^{-1/2}$ arises through $\xi(T)$, independently of M. Unfortunately, in practice it is difficult to directly measure $m(T, B)$ for a (Ga,Mn)As film due to the diamagnetic background from the GaAs substrate. Thus, in our analysis we have chosen to represent the magnetization at any given temperature and field by the Brillouin function with $J = 5/2$, since this is generally accepted as a good approximation. In Fig. 4(a) we have plotted the calculated am^2 for $B = 6$ T (dashed curve) for comparison. Clearly, the magnetization calculated from the Brillouin function is generally in good agreement with $A(m) = \sigma_{xx} - C - B(T)$ derived from Eq. (8) except that it decreases slowly at intermediate temperature (between 10 K and T_C) due to our inability to account for thermal excitations of magnons in the calculation[39].

Having established $m(T, B)$ via Fig. 4(a), we now address the temperature dependence of σ_{xy}. In Fig. 4(b), we plot σ_{xy} as a function of temperature for the same sample at 6 T, which shows only a magnetization-like curve, with no cusp around T_C, suggesting the absence of quantum corrections to the anomalous Hall conductivity σ_{xy}, consistent with the results reported by Mitra *et al.*[19] Additionally, by carefully comparing the anomalous Hall conductivity σ_{xy} and magnetization m, we find that σ_{xy} drops much more slowly than m above T_C, in contrast to the general belief that σ_{xy} is simply proportional to the magnetization. For clarification, we plot $\sigma_{xy}/m \approx \chi_S M_0$ (where M_0 is the value of M at low T, i.e., a fixed quantity for each sample) as a function of temperature in Fig. 4(b), which clearly shows that the anomalous Hall coefficient χ_S is not a constant, but increases rapidly with T at temperatures above T_C. A possible explanation for this behavior can be found by introducing the Berry phase[5], which has been shown to exist in the closely related system (In,Mn)Sb[40], into the present context. However, this requires further examination.

C. Temperature dependence of scaling relations

Since AHE may originate from either intrinsic or extrinsic mechanisms characterized by different exponential factors n in the scaling relations between the anomalous Hall and longitudinal resistivities, it is informative to examine the relation between ρ_{xx} and ρ_{xy} instead of σ_{xx} and σ_{xy} as the temperature varies, in order to determine these exponential factors n. We therefore address the temperature variation of the transport data by examining the scaling relationship of the form $\rho_{xy} \sim \rho_{xx}^n$ by considering the temperature dependence of the magnetization. Conventional theory predicts the value of $n = 2$ for the intrinsic mechanism inherited from spin-orbit-coupled Bloch bands[5]; and for extrinsic
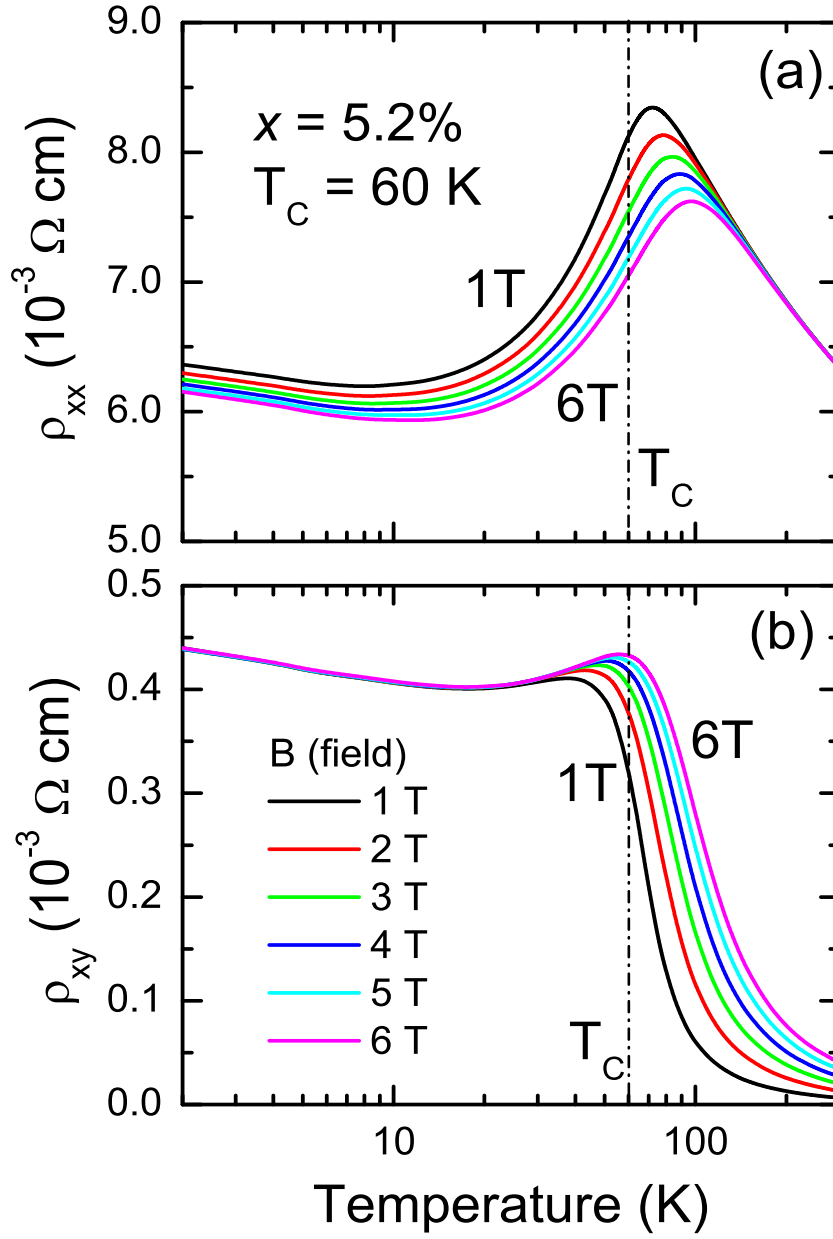
FIG. 3: (Color online) (a) and (b), the temperature dependences of longitudinal and transverse resistivities ρ_{xx} and ρ_{xy} of a typical 99 nm thick $Ga_{0.948}Mn_{0.052}As$ sample at several magnetic fields.

mechanisms, $n = 1$ is predicted for skew scattering[2] and $n = 2$ for the side jump process[3]. In recent experiments[9], a scaling factor of $n = 2$ has been reported for metallic (Ga,Mn)As samples at low temperatures. However, the origin of this scaling – whether it comes about from side jump or from the intrinsic mechanism – is still under vigorous discussion and requires further inquiry.
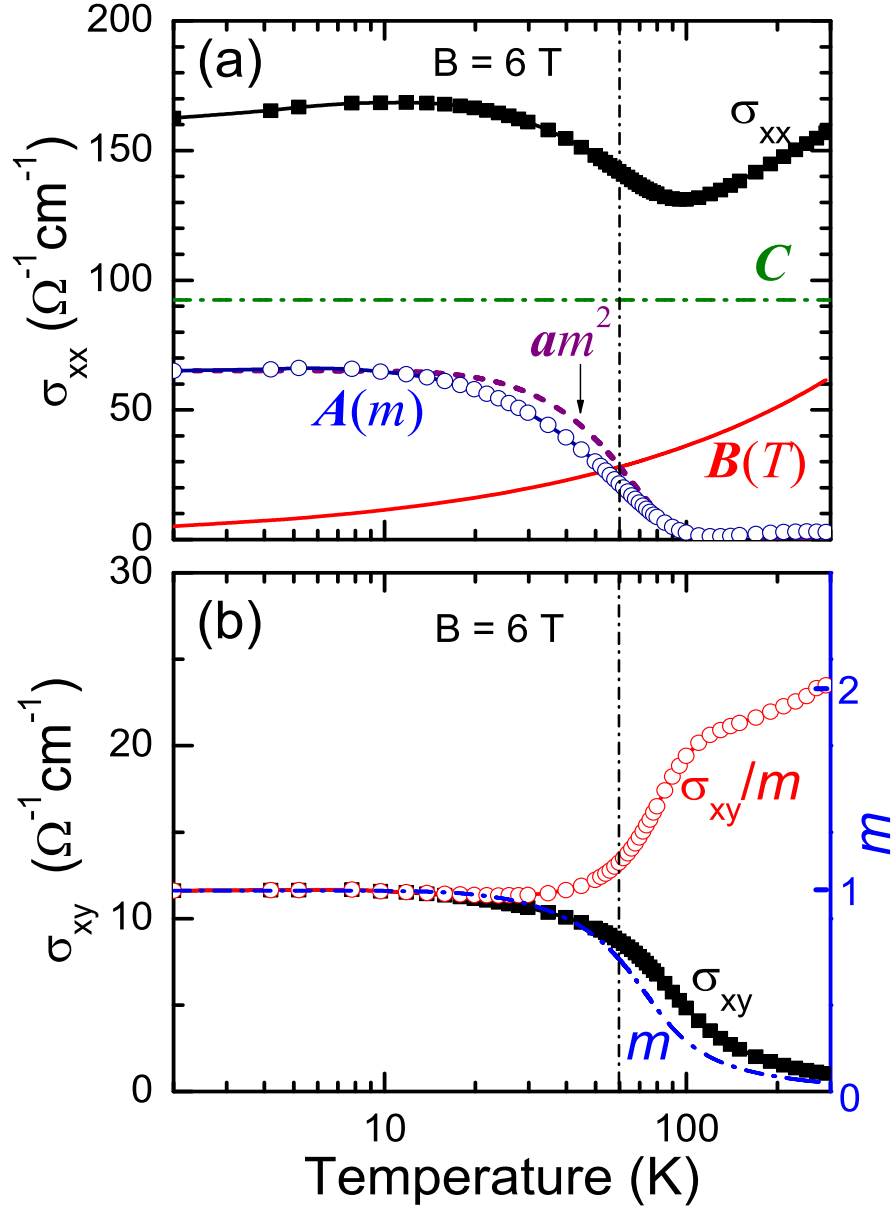
FIG. 4: (Color online) (a) The temperature dependences of σ_{xx} (solid black squares), C (dash-dotted blue line), $A(m)$ (open dark blue circles), $B(T)$ (solid red curve) and calculated am^2 (dashed purple curve) at 6 T. (b) The temperature dependences of σ_{xy} (solid black squares), calculated m (dash-doted blue line) and σ_{xx}/m (open red circles) at 6 T.

1. Scaling relations for ρ_{xy} vs. ρ_{xx} from their temperature dependence

We first examine the relation between ρ_{xy}/m and ρ_{xx} for all samples by constructing a logarithmic plot of ρ_{xy}/m vs. ρ_{xx}. Quite surprisingly, a *universal behavior* is observed in Fig. 5 – two linear ranges with approximately the same slope are shown in the logarithmic plot, one at temperatures below 10 K, and the other for high temperatures, far above T_C. For easy identification, we have indicated the Curie temperature for each sample by the point shown on each

curve, the locus of which is the line of demarcation between the low ($T < T_C$) and high ($T > T_C$) temperatures region. Note that the latter region has not been carefully investigated before, but is in fact quite important for two reasons: the fundamental interest of how the "residue" of ferromagnetism behaves above T_C; and for extracting the value of hole concentration at high temperatures from Hall measurements, a process that is frequently used as a measurement of p in (Ga,Mn)As. The linear fitting of our data for this region yields the exponential factor n of around 1.8 to 2.0 for most samples despite the fact that each sample has a different resistivity, Mn concentration, Curie temperature, and magnetization, as shown in Table I. It should be emphasized that – although from the plots the scaling relation cannot be extracted for the intermediate temperature range – we can attribute this to the temperature variation of the anomalous Hall coefficient χ_S, which increases monotonically in this range as the temperature increases. This conjecture is justified by the points indicating the Curie temperature in Fig. 5, which form a line with a similar slope as the data at low temperature. Note that in a logarithmic plot of ρ_{xy} vs. ρ_{xx} the linear fit with $n \sim 2$ can only be obtained for low temperatures, but a well-defined relation between ρ_{xy} and ρ_{xx} cannot be found as the temperature increases beyond some value specific for each sample. Our data therefore confirm that the scaling relation between ρ_{xy} and ρ_{xx} (and therefore also between σ_{xy} and σ_{xx}) breaks down at high temperatures, but the scaling relation of $\rho_{xy}/m = \chi_S(T)\rho_{xx}^n M_0$ with $n = 2$ does apply (including temperatures above T_C), provided that we allow χ_S to depend on temperature.

2. Scaling relations for σ_{xy} vs. σ_{xx} from temperature-dependent measurements

To gain additional insight into AHE, we now attempt to interpret the scaling relation of $\rho_{xy}/m = \chi_S(T)\rho_{xx}^n M_0$ with $n = 2$ in terms of the transverse and longitudinal conductivity. In Fig. 6(a), we plot $\sigma_{xy}/m = \chi_S(T)M_0$ as function of $m(T, B)$ for all studied samples at $B = 6$ T. Figure 6(a) clearly shows that χ_S is actually a more straightforward function of m than of T, as seen by comparing it with the plot of σ_{xy}/m vs. T in Fig. 4(b). More evidently, if we normalize each σ_{xy}/m curve by its zero-temperature value (i.e., its value at $m = 1$ on the graph), all curves except those for the two samples with the smallest thicknesses (10 nm) collapse into nearly a single curve, as shown in Fig. 6(b). Considering the fact that $m(T, B)$ calculated using the Brillouin function with $J = 5/2$ is systematically higher than the actual magnetization in the intermediate temperature range (between 10 K and T_C) – which is believed to be the reason for the concave shape of σ_{xy}/m in Fig. 6 – suggests a linear relation,

$$\chi_S(m) = \chi_S(1) + \beta\chi_S(1)(1 - m). \tag{9}$$

Here $\beta = [\chi_S(0) - \chi_S(1)]/\chi_S(1) \approx 1$, so that the anomalous Hall conductivity varies as $\sigma_{xy} \propto M + \beta M(1 - m)$ with $\beta \approx 1$. A similar relation, $\sigma_{xy} \propto M(1 - \alpha M)$, where α is a constant, has been predicted theoretically on the basis of the Berry phase[5], and confirmed in (In,Mn)Sb by studying the field dependent anomalous Hall effect[40]. Such relationship was explained by assuming that as the field is varied, the relative position of the bands shifts linearly with the absolute value of the magnetization (due to exchange splitting), thus resulting in the anomalous Hall coefficient which will also be linear with M. Unfortunately we cannot confirm this explanation, since we did not observe the field dependent anomalous Hall coefficient up to 6 T in this study directly.

A temperature dependent anomalous Hall coefficient $\chi_S(T)$ is expected, since the absolute value of the magnetization drops with increasing temperature, although to date this has never been carefully explored. Here it should be emphasized that a universal value of $\beta \approx 1$ obtained in this work is not expected in metallic (Ga,Mn)As, i.e., it is not predicted by any existing theory of the AHE. Although we cannot rule out the possible explanation of temperature dependent χ_S based on the Berry phase theory, here we propose – based on the behavior seen in Figs. 5 and 6 – an alternative explanation, that there are two mechanisms contributing to anomalous Hall coefficient χ_S with the *same order* of magnitude. One mechanism (corresponding to the convergence of the ρ_{xy} vs. ρ_{xx} plots in the lower part of the panels in Fig. 5) has a weak temperature dependence and dominates at low temperatures, showing an exponent n of about 2 in the relation $\rho_{xy} \propto \rho_{xx}^n$ (see Table I). We can ascribe this scaling relation as arising either from intrinsic or from side-jump processes. The other (corresponding to the convergence of the plots in the upper part of the panels) can probably be associated with magnetization fluctuations[41]. In the latter case, because of the presence of fluctuations, we will naturally expect term such as $M_0 - M(T)$ (i.e., $M_0(1 - m)$) or $M_0^2 - M^2(T)$, which emerges at higher temperatures.

It should be emphasized that, as shown in Fig. 6, we see that the temperature (or magnetization) dependences of the normalized values of σ_{xy}/m behave similarly for all samples with thicknesses ranging from 20 nm to 100 nm and Mn concentrations from 3.9% to 6.7%, (i.e, they collapse into an overlapping single group of curves), but the two thinnest samples (the as-grown and annealed 10 nm samples) conspicuously deviate from the behavior of the thicker specimens. We therefore believe that our conclusion is valid for bulk-like film, i.e., there is no effect of thickness and Mn concentration on the temperature dependence of σ_{xy} in thick films. This suggests that the deviation seen in the
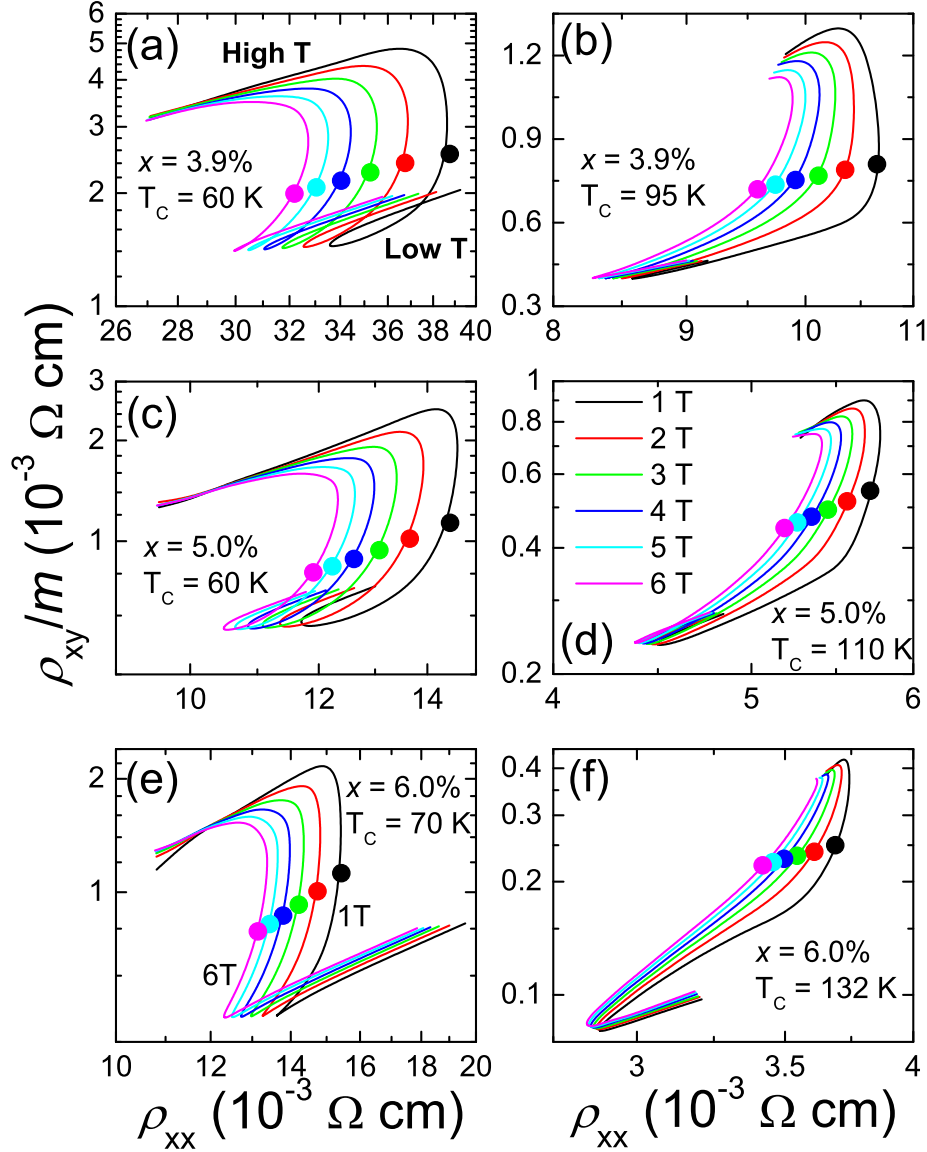
FIG. 5: (Color online) Logarithmic plots of ρ_{xy}/m vs. ρ_{xx} at various temperatures $(2-300$ K$)$ and magnetic fields $(1-6$ T$)$ for three as-grown samples, (a), (c), (e); and three annealed samples, (b), (d), (f). The shift of curves at low temperature with varying magnetic field is attributed to the ordinary Hall effect. The points in the figure indicate the Curie temperature for each sample.

case of the ultrathin samples ($t < 10$ nm) signals a process that is not accounted for in our analysis, and may be associated with an emergence of surface effects or from a significant contribution of quantum confinement.

We note parenthetically that transport measurements are sensitive to local microscopic inhomogeneities. And from our early neutron reflection measurements[42], we were able to establish that there exists some magnetic inhomogeneity along the growth direction, which is especially evident in as-grown samples. In that work it was also shown that low temperature annealing dramatically reduces such inhomogeneity. Furthermore, this improvement of homogeneity in annealed GaMnAs was demonstrated independently by the annealing-induced reduction of the resonance linewidth in ferromagnetic resonance (FMR) measurements[43]. Since the behavior which we report in the present paper is similar for both as-grown and annealed samples, this therefore leads us to believe that the observation of the two
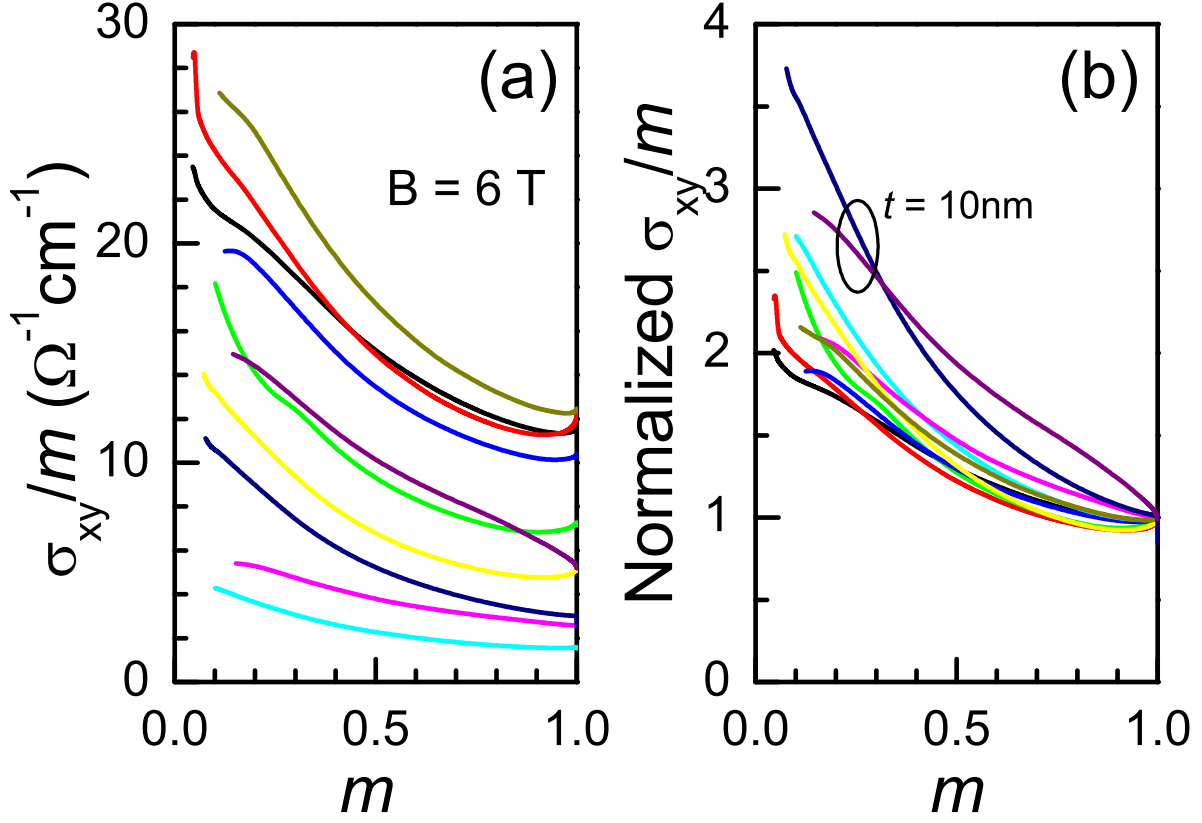
FIG. 6: (Color online) (a) $\sigma_{xy}/m = \chi_S(T)M_0$ vs. $m(T,B)$ are plotted for all studied samples at $B = 6$ T. (b) σ_{xy}/m normalized by its value at $m = 1$ vs. $m(T,B)$ are plotted for all studied samples at $B = 6$ T. Two samples with the thinnest thickness are marked in the figure.

contributions to AHE is not related to local microscopic inhomogeneities (or nonuniformity), but rather to thermal magnetic fluctuations. Note that spin fluctuations at the phase transition, i.e., an increase of scattering ("de-phasing") due to spin disorder, were also reported as an increase of the FMR linewidth near the Curie temperature in (Ga,Mn)As system[43,44].

D. The connection between scaling relations and the metal-insulator transition

We now summarize and discuss the magneto-transport results obtained in metallic (Ga,Mn)As. At near zero temperature, despite the fact that the particular samples may differ in magnetization values and/or hole concentrations, we find that a surprisingly universal empirical scaling relation exists between the Hall and longitudinal conductivities $\sigma_{xy} \propto \sigma_{xx}^{1.5}$ (i.e., $\rho_{xy} \propto \rho_{xx}^{0.5}$) in the range of low hole concentration (p up to 10^{20} cm^{-3}), i.e., near the Anderson-Mott metal-insulator transition point. However, such scaling relation is broken as p increases, revealed by the very different behaviors of σ_{xy} and σ_{xx} in Figs. 1(a) and 1(b) when p exceeds 10^{20} cm^{-3}. On the other hand, from the temperature dependences of σ_{xy} and σ_{xx} observed in individual samples, we find that another scaling relation exists for each sample, $\rho_{xy} \propto \rho_{xx}^2$ (i.e., $\sigma_{xy} = \rho_{xy}/\rho_{xx}^2 \approx \chi_S M$, with no direct relation to σ_{xx}) in the very low temperature range, but quickly breaks down with increasing temperature. However, by introducing a normalized magnetization parameter $m(T,B)$ calculated from the Brillouin function, we are able to establish a new scaling relation: $\rho_{xy}/m = \chi_S(m)\rho_{xx}^2 M_0$, which leads to a magnetization-dependent anomalous Hall coefficient $\chi_S(m) = \chi_S(1) + \beta\chi_S(1)(1-m)$, where $\beta \approx 1$.

Clearly these two scaling relations for low temperatures – one obtained from all samples at a fixed temperature, and the other from temperature-dependent magnetotransport measured on individual samples – coexist and disagree with each other in the low p range (up to 10^{20} cm^{-3}). This incongruity cannot be explained by the model provided by Onoda *et al.*[33,34], in which three scaling relations are predicted in different conductivity regimes depending on the carrier scattering time.

As an "*ad hoc*" attempt, however, this disagreement can be resolved to some extent by introducing the relation $M_0 \propto \sigma_{xx}^{1.5}$ – which, based on the power-law relation between $\sigma_{xx} \propto (p-p_c)^{0.5}$ shown in Fig. 2(a), automatically implies the interesting result that $M_0 \propto (p-p_c)^{0.75}$. We will return to this point below. Consequently, we now have a new scaling relation $\rho_{xy}/(p-p_c)^{0.75} \propto \rho_{xx}^2$ for (Ga,Mn)As in the intermediate conductivity range ($30\ \Omega^{-1}$cm$^{-1} < \sigma_{xx} < 100\ \Omega^{-1}$cm^{-1}) at near zero temperature, which is very similar to the relation $\rho_{xy}/p^{2/3} \propto \rho_{xx}^2$ predicted and confirmed by either the Berry phase[9] or the side jump[19] models. However, this scaling relation fails in both the localized ($p < p_c$) and the highly conducting regimes ($\sigma_{xx} > 100\ \Omega^{-1}$cm^{-1})[14].

The results presented above show that the physics of conductivity, AHE and magnetization are dominated by the nature of the Anderson-Mott metal-insulator transition. Close to the critical hole concentration p_c, in the conducting regime, σ_{xx}, σ_{xy}, and M_0 all have the power law form $(p-p_c)^s$ where, based on a simplified 3-dimensional localization model, s is expected to be of order of unity for all these three physical quantities σ_{xx}, σ_{xy}, and M_0. If the exponent s is the same for all three quantities, this leads to two relations: $\sigma_{xy} \propto \sigma_{xx}$ and $\sigma_{xy} \propto M_0$. The former relation is incompatible with our observations, while the latter contains a natural explanation for a scaling relation $\rho_{xy}/M_0 \propto \rho_{xx}^2$. In fact, our results suggests that the exponent s is different for σ_{xy} and σ_{xx} near the critical regime (e.g., $s \approx 0.76$ for σ_{xy}, and 0.5 for σ_{xx}), leading to a universal scaling relation $\sigma_{xy} \propto \sigma_{xx}^\gamma$ with $\gamma \sim 1.5 \neq 1$ for intermediately conductivity (Ga,Mn)As samples ($\sigma_{xx} < 100\ \Omega^{-1}$cm^{-1}). To some extent the above conjecture agrees with the theoretical model based on the Keldysh formalism, recently developed for multiband ferromagnetic metals by Onoda *et al.*[33,34] However, future theoretical investigations in connection with the Anderson-Mott localization model are required to justify our conjecture, $M_0 \propto (p-p_c)^{0.75}$, for resolving the issue of coexistence of the two apparently contradictory scaling relations in the region below $p - p_c = 1 \times 10^{20}$ cm^{-3}.

Furthermore, we should emphasize that in the picture of localization the saturation magnetization at zero temperature M_0 (which was shown to obey a power law $(p - p_c)^{0.75}$) becomes a function of disorder, and therefore ceases to be simply proportional to the Mn concentration. This implies two important phenomena: First, our experiment suggests that M_0 has the same exponent s as σ_{xy}, which is around 0.76 ± 0.06 in our samples in the intermediate conducting regime ($30\ \Omega^{-1}$cm$^{-1} < \sigma_{xx} < 100\ \Omega^{-1}$cm^{-1}), coincidentally close to the exponent of $2/3$ used in previous analyses[9,19]. However, both M_0 and σ_{xy} deviate from this power-law form in highly conducting samples ($\sigma_{xx} > 100\ \Omega^{-1}$cm^{-1}), which leads to the unanticipated dependence of M_0 and σ_{xy} on the hole concentration[14]. Second, near the metal-insulator transition, M_0 and σ_{xy} at zero temperature should decrease as p decreases toward p_c, and should eventually vanish in the localized regime, as predicted by the theory of AHE in ferromagnetic (Ga,Mn)As in the regime where conduction is due to phonon-assisted hopping of holes between localized states in the impurity band[45]. As a result, we speculate that there exists another phase transition as the temperature approaches zero in an insulating ferromagnetic (Ga,Mn)As sample. This provides special motivation to extend measurements of magnetization to ultra-low temperatures.

Generally, electron localization might arise from disorder (Anderson transition) or from electron-electron interactions (Mott-Hubbard transition)[46]. Therefore, the different temperature variations of σ_{xx} and σ_{xy} might indicate that both features play a role in conductivity σ_{xx}, but the anomalous Hall conductivity σ_{xy} is only affected by the hole concentration p, which is indirectly related to disorder[46], i.e., the statistical distribution of dopant atoms in the crystalline host. This might offer a natural explanation for the different exponents observed for σ_{xx} and σ_{xy}, which leads to a universal empirical scaling relation $\sigma_{xy} \propto \sigma_{xx}^\gamma$ with $\gamma \sim 1.5$ around the critical point.

IV. SUMMARY AND CONCLUSIONS

In this paper we carried out a systematic study of the dependences of the longitudinal (σ_{xx}) and transverse anomalous Hall (σ_{xy}) conductivities on the hole concentration and temperature in a series of ten metallic (Ga,Mn)As samples with different hole and Mn concentrations. The entire series covered the conductivity range of $30\ \Omega^{-1}$cm$^1 < \sigma_{xx} < 300\ \Omega^{-1}$cm^{-1} and hole concentration range 3.6×10^{19} cm$^{-3} < p < 7.3 \times 10^{20}$ cm^{-3}. We summarize our results below.

Transport data taken near zero temperature on the entire series of the GaMnAs samples has allowed us to establish a scaling relation – $\sigma_{xy} \propto \sigma_{xx}^{1.5}$ – which holds in the conductivity range $30\ \Omega^{-1}$cm$^1 < \sigma_{xx} < 100\ \Omega^{-1}$cm^{-1} (corresponding to 3.6×10^{19} cm$^{-3} < p < 1.0 \times 10^{20}$ cm^{-3}), which we refer to as the "intermediate" conductivity range. However, this relation was found to break down in the high conductivity limit ($\sigma_{xx} > 100\ \Omega^{-1}$cm^{-1}).

At the same time, a scaling relation – $\rho_{xy} \propto \rho_{xx}^2$ – was established from the temperature variation of the transport data observed at low temperatures ($T < 10$ K) individually on all samples of the series. This relation, however fails

at high temperatures.

While the two relations, $\sigma_{xy} \propto \sigma_{xx}^{1.5}$ and $\rho_{xy} \propto \rho_{xx}^2$, are found to hold in the *same* conductivity and temperature range (30 Ω^{-1}cm^{-1} < σ_{xx} < 100 Ω^{-1}cm^{-1}; T < 10 K), they are contradictory, and need to be reconciled.

In order to reconcile this inconsistency, we find that a universal scaling relationship $\rho_{xy}/M_0 \propto \rho_{xx}^2$ can be established in connection with the Anderson-Mott metal-insulator transition. In accomplishing this, we find that both M_0 and σ_{xy} must obey the power law form of $(p - p_c)^s$ with the same exponent s in the intermediate conductivity regime (30 Ω^{-1}cm^{-1} < σ_{xx} < 100 Ω^{-1}cm^{-1}, and p ranging from $p_c \approx 2.8 \times 10^{19}$ cm^{-3} to $\sim 1.0 \times 10^{20}$ cm^{-3}).

We emphasize that this "reconciliation" leads to the surprising result that M_0 variation is determined by a power of $(p - p_c)$.

In order to explain the observed temperature dependence of AHE up to high temperatures (including $T > \mathrm{T}_C$), we also establish a scaling relationship $\rho_{xy}/m \propto \rho_{xx}^n$, with $n \approx 2.0$, where $m = M(T, B)/M_0$. As a result, we find that the anomalous Hall coefficient χ_S itself depends on the magnetization, which suggests that the temperature dependence of σ_{xy} can be attributed to two contributions: a contribution from either intrinsic or side-jump process, which dominates at low temperature; and another which emerges at high temperatures as the magnetization fluctuations quickly escalate. It is still not certain which process (intrinsic or side-jump) is dominant at low temperatures.

It is interesting that the effect of two entirely different contributions to the anomalous Hall coefficient χ_S – that arising from the intrinsic or side jump processes and that induced by magnetization fluctuation – have the same order of magnitude. Resolving the reasons for this should lead to a better understanding of the physics of AHE in GaMnAs.

Acknowledgments

[*] Electronic address: `xliu2@nd.edu`

[†] Electronic address: `slee3@korea.ac.kr`

[1] G. Bergmann, Physics Today **32**, 25 (1979).

[2] J. Smit, Physica **21**, 877 (1955).

[3] L. Berger, Phys. Rev. B **2**, 4559 (1970).

[4] V. K. Dugaev, A. Crépieux, and P. Bruno, Phys. Rev. B **64**, 104411 (2001).

[5] T. Jungwirth, Q. Niu, and A. H. MacDonald, Phys. Rev. Lett. **88**, 207208 (2002).

[6] S. Onoda, N. Sugimoto, and N. Nagaosa, Phys. Rev. Lett. **97**, 126602 (2006).

[7] N. Nagaosa, J. Sinova, S. Onoda, A. H. MacDonald, and N. P. Ong, Rev. Mod. Phys. **82**, 1539 (2010).

[8] J. Cumings, L. S. Moore, H. T. Chou, K. C. Ku, G. Xiang, S. A. Crooker, N. Samarth, and D. Goldhaber-Gordon, Phys. Rev. Lett. **96**, 196404 (2006).

[9] S. H. Chun, Y. S. Kim, H. K. Choi, I. T. Jeong, W. O. Lee, K. S. Suh, Y. S. Oh, K. H. Kim, Z. G. Khim, J. C. Woo, and Y. D. Park, Phys. Rev. Lett. **98**, 026601 (2007).

[10] Y. Pu, D. Chiba, F. Matsukura, H. Ohno, and J. Shi, Phys. Rev. Lett. **101**, 117208 (2008).

[11] Y. Tian, L. Ye, and X. Jin, Phys. Rev. Lett. **103**, 087206 (2009).

[12] W. Jiang, A. Wirthmann, Y. S. Gui, X. Z. Zhou, M. Reinwald, W. Wegscheider, C.-M. Hu, and G. Williams, Phys. Rev. B **80**, 214409 (2009).

[13] M. Glunk, J. Daeubler, W. Schoch, R. Sauer, and W. Limmer, Phys. Rev. B **80**, 125204 (2009).

[14] D. Chiba, A. Werpachowska, M. Endo, Y. Nishitani, F. Matsukura, T. Dietl, and H. Ohno, Phys. Rev. Lett. **104**, 106601 (2010).

[15] J. Ye, Y. B. Kim, A. J. Millis, B. I. Shraiman, P. Majumdar, and Z. Tešanović, Phys. Rev. Lett. **83**, 3737 (1999).

[16] K. Ohgushi, S. Murakami, and N. Nagaosa, Phys. Rev. B **62**, R6065 (2000).

[17] M. Onoda and N. Nagaosa, J. Phys. Soc. Jpn. **71**, 19 (2002).

[18] F. D. M. Haldane, Phys. Rev. Lett. **93**, 206602 (2004).

[19] P. Mitra, N. Kumar, and N. Samarth, Phys. Rev. B **82**, 035205 (2010).

[20] S. Shen, X. Liu, Z. Ge, J. K. Furdyna, M. Dobrowolska, and J. Jaroszynski, J. Appl. Phys. **103**, 07D134 (2008).

[21] A. Richardella, P. Roushan, S. Mack, B. Zhou, D. A. Huse, D. D. Awschalom, Ali Yazdani, Science **327**, 665 (2010).

[22] K. C. Ku, S. J. Potashnik, R. F. Wang, M. J. Seong, E. Johnston-Halperin, R. C. Myers, S. H. Chun, A. Mascarenhas, A. C. Gossard, D. D. Awschalom, P. Schiffer, and N. Samarth, Appl. Phys. Lett. **82**, 2302 (2003).

[23] A. H. MacDonald, P. Schiffer, and N. Samarth, Nature Mater. **4**, 195 (2005).

[24] K. M. Yu, W. Walukiewicz, T. Wojtowicz, I. Kuryliszyn, X. Liu, Y. Sasaki, and J. K. Furdyna, Phys. Rev. B **65**, 201303(R) (2002).

[25] K. M. Yu, W. Walukiewicz, T. Wojtowicz, J. Denlinger, M. A. Scarpulla, X. Liu, and J. K. Furdyna, Appl. Phys. Lett. **86**, 042102 (2005).

[26] M. A. Paalanen, T. F. Rosenbaum, G. A. Thomas, and R. N. Bhatt, Phys. Rev. Lett. **48**, 1284 (1982).

[27] T. F. Rosenbaum, R. F. Milligan, M. A. Paalanen, G. A. Thomas, R. N. Bhatt, and W. Lin, Phys. Rev. B **27**, 7509 (1983).

[28] F. Wegner, Z. Phys. B **25**, 327 (1976).

[29] P. A. Lee, and T. V. Ramakrishnan, Rev. Mod. Phys. **57**, 287 (1985).

[30] H. Stupp, M. Hornung, M. Lakner, O. Madel, and H. v. Löhneysen, Phys. Rev. Lett. **71**, 2634 (1993); *ibid*. **72**, 2122 (1994).

[31] S. Waffenschmidt, C. Pfleiderer, and H. v. Löhneysen, Phys. Rev. Lett. **83**, 3005 (1999).

[32] T. Fukumura, H. Toyosaki, K. Ueno, M. Nakano, T. Yamasaki, and M. Kawasaki, Japanese J. Appl. Phys. **46**, L642 (2007).

[33] S. Onoda, N. Sugimoto, and N. Nagaosa, Phys. Rev. Lett. **97**, 126602 (2006).

[34] S. Onoda, N. Sugimoto, and N. Nagaosa, Phys. Rev. B **77**, 165103 (2008).

[35] F. Matsukura, H. Ohno, A. Shen, and Y. Sugawara, Phys. Rev. B **57**, R2037 (1998).

[36] C. P. Moca, B. L. Sheu, N. Samarth, P. Schiffer, B. Janko, and G. Zarand, Phys. Rev. Lett. **102**, 137203 (2009).

[37] D. Belitz and K. I. Wysokinski, Phys. Rev. B **36**, R9333 (1987).

[38] This approximation may be too rough for (Ga,Mn)As around T_C, given that ξ is function of both $g_0(m)$ and temperature T, see Ref. 36.

[39] Charles Kittel, *Introduction to Solid State Physics* (Wiley: New York, 2004).

[40] G. Mihály, M. Csontos, S. Bordács, I. Kézsmarki, T. Wojtowicz, X. Liu, B. Jankó and J. K. Furdyna, Phys. Rev. Lett. **100**, 107201 (2008).

[41] Yu. P. Irkhin and Sh. Sh. Abelskii, Soviet Phys. – Solid State **6**, 1283 (1964).

[42] B. J. Kirby, J. A. Borchers, J. J. Rhyne, S. G. E. te Velthuis, A. Hoffmann, K. V. O'Donovan, T. Wojtowicz, X. Liu, W. L. Lim, and J. K. Furdyna, Phys. Rev. B **69**, 081307(R) (2004).

[43] X. Liu, Y. Sasaki, J. K. Furdyna, Phys. Rev. B 67, 205204 (2003).

[44] X. Liu and J. K. Furdyna, J. Phys.: Condens. Matter **18**, R245-279 (2006).

[45] A. A. Burkov and L. Balents, Phys. Rev. Lett. **91**, 057202 (2003).

[46] D. Belitz and T. R. Kirkpatrick, Rev. Mod. Phys. **66**, 261 (1994).